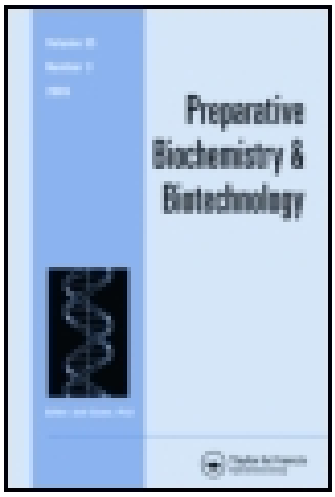

Preparative Biochemistry and Biotechnology
Publication details, including instructions for authors and subscription information:
http://www.tandfonline.com/loi/lpbb20

Deletion of the budBAC Operon in Klebsiella pneumoniae to Understand the Physiological Role of 2,3-butanediol Biosynthesis

Daun Jeong[a], Jeongmo Yang[a], Soojin Lee[a], Borim Kim[a], Youngsoon Um[b], Youngrok Kim[c], Kyoung-Su Ha[a] & Jinwon Lee[a]

[a] Department of Chemical and Biomolecular Engineering, Sogang University, Seoul, South Korea

[b] Korea Clean Energy Center, Korea Institute of Science and Technology, Seoul, South Korea

[c] Institute of Life Sciences and Resources, and Department of Food Science and Biotechnology, Kyung Hee University, Yongin, South Korea

Accepted author version posted online: 15 Jul 2015.

To cite this article: Daun Jeong, Jeongmo Yang, Soojin Lee, Borim Kim, Youngsoon Um, Youngrok Kim, Kyoung-Su Ha & Jinwon Lee (2015): Deletion of the budBAC Operon in Klebsiella pneumoniae to Understand the Physiological Role of 2,3-butanediol Biosynthesis, Preparative Biochemistry and Biotechnology, DOI: 10.1080/10826068.2015.1045603

To link to this article: http://dx.doi.org/10.1080/10826068.2015.1045603

Deletion of the *budBAC* operon in *Klebsiella pneumoniae* to understand the physiological role of 2,3-butanediol biosynthesis

Daun Jeong[1], Jeongmo Yang[1], Soojin Lee[1], Borim Kim[1], Youngsoon Um[2], Youngrok Kim[3], Kyoung-Su Ha[1], Jinwon Lee[1]

[1]Department of Chemical and Biomolecular Engineering, Sogang University, Seoul, South Korea,
[2]Korea Clean Energy Center, Korea Institute of Science and Technology, Seoul, South Korea,
[3]Institute of Life Sciences and Resources, and Department of Food Science and Biotechnology, Kyung Hee University, Yongin, South Korea

E-mail: jinwonlee@sogang.ac.kr

Daun Jeong and Jeongmo Yang contributed equally to this work.

Abstract

Klebsiella pneumoniae is known to produce 2,3-butanediol (2,3-BDO), a valuable chemical. In *K. pneumoniae*, the 2,3-BDO operon (*budBAC*) involved in the production of 2,3-BDO. To observe the physiological role of the 2,3-BDO operon in a mixed acid fermentation, we constructed a *budBAC* deleted strain (SGSB109). The production of extracellular metabolites, CO_2 emission, carbon distribution, and NADH/NAD^+ balance of SGSB109 were compared with the parent strain (SGSB100). When comparing the carbon distribution at 15h period, four significant differences were observed; 2,3-BDO biosynthesis, lactate and acetate production (lactate and acetate production increased 2.3-fold and 4.1-fold in SGSB109 compared to SGSB100), CO_2 emission (higher in SGSB100), and carbon substrate uptake (higher in SGSB100). Previous studies on the inactivation of 2,3-BDO operon were focused on the increase of 1,3-propandiol

production. Few studies were done on observing the role of 2,3-BDO biosynthesis. This study provides a prime insight in the role of 2,3-BDO biosynthesis of *K. pneumoniae*.

KEYWORDS: 2,3-butanediol, budBAC operon, carbon distribution analysis, CO_2 emission, redox balance

INTRODUCTION

Owing to the current exhaustion of fossil fuel supplies and unstable petroleum prices, bio-based chemical compounds and microbial production of these chemicals are receiving significant interest globally. 2,3-BDO, one of promising candidates for microbial production, is a platform chemical that can be converted into several industrial chemicals via simple chemical reactions. For example, 1,3-butandiene, which is an organic intermediate for synthetic rubber production and which is generally obtained from crude oil, is a major derivative of 2,3-BDO. For these reasons, microbial production of 2,3-BDO has been intensively studied in recent years. [1, 2, 3] A number of species in the genera *Klebsiella*, *Bacillus*, *Serratia* and *Pseudomonas* can produce 2,3-BDO via their own carbohydrate metabolism. Among these species, *Klebsiella pneumoniae*, a gram-negative bacterium in the family *Enterobacteriaceae*, is a potentially useful industrial producer because of its wide substrate spectrum, high efficiency, and ease of culturing.[4] However, because *K. pneumoniae* is a risk-group 2 organisum, alleviation of the *Kebsiella* pathogenicity has been carried out prior to this experiment.

K. pneumoniae produces 2,3-BDO from pyruvate, which is produced in a relatively simple manner via the Embden-Meyerhof pathway (EMP), using glucose as a carbon substrate. Following EMP (also known as glycolysis), two molecules of pyruvate are converted to 2,3-BDO via three chemical reactions facilitated by the enzymes α-acetolactate synthase (*budB*), α-acetolactate decarboxylase (*budA*), and acetoin reductase (*budC*). Genes encoding 2,3-BDO-producing enzymes are contained within an operon (called the *budBAC* operon) in the *K. pneumoniae* chromosome, and expression of this operon is regulated by *budR*, which is a LysR-type transcriptional regulator gene. Currently, studies of microbial 2,3-BDO production are progressing rapidly, and typically take one of three main perspectives: elimination of pathogenic characteristics of *K. pneumoniae*, enhancement of 2,3-BDO production, and widening of the spectrum of available carbon substrates.

Enhancement of 2,3-BDO production has mainly progressed by the disruption of genes participating in by-product formation and the over-expression of genes related to 2,3-BDO biosynthesis. For example, in a recent study, the *ldhA* gene, which is involved in biosynthesis of lactate (a by-product of 2,3-BDO production), was disrupted and *budB* and *budA* genes involved in 2,3-BDO biosynthesis were overexpressed; 111.3 g/L of 2,3-BDO was produced with a productivity of 2.71 g/L · h in fed-batch fermentation.[5] To widen the carbon substrate spectrum for 2,3-BDO production, several studies have been performed on utilization of by-product carbon sources generated by industrial processes. For example, in a recent study, corncob molasses, a waste by-product of xylitol production that contains high concentrations of mixed sugars, was utilized for 2,3-BDO

production. After 61 h of fed-batch fermentation using corncob molasses as a carbon substrate, a maximum 2,3-BDO concentration of 78.9 g/L was achieved, along with a productivity of 1.3 g/L · h, and a yield of 81.4%.[6] Also, there are several previous studies on 2,3-BDO production by gas as the carbon source; 2.38 g/L of 2,3-BDO production by cyanobacteria using CO_2, and 2,3-BDO production by *Clostridium* species using carbon monoxide containing industrial waste gases or syngas.[7, 8] These papers show that the production of 2,3-BDO from various carbon sources is possible using a non-pathogenic strains.

Most previous research on 2,3-BDO biosynthesis has been conducted with an industrial perspective, rather than a physiological or biochemical approach. Topics related to the fundamental purpose and meaning of 2,3-BDO production in *Klebsiella sp*. have not been intensively studied. In this study, by comparing two strains (SGSB100(Δ*wabG*) and SGSB109(Δ*wabG*Δ*budBAC*)) we observed the primary role and meaning of 2,3-BDO biosynthesis in *K. pneumoniae* at a mixed fermentation condition. Also, several metabolic engineering techniques were used to illuminate the meaning of 2,3-BDO biosynthesis in *K. pneumoniae*.

MATERIALS AND METHODS

Development Of Strains And Plasmids

The strains, plasmids, and primers used in this study are listed in Table 1.[9] The *budA*, *budB* and *budC* genes were derived from *K. pneumoniae* KCTC2242 (Korean Collection for Type Culture). *Escherichia coli* DH5α [F-(80d *lacZ* M15) (*lacZYA*-rgF)U1691

hsdR17(m+)*recA1 endA1 relA1 deoR*; Dong In Biotech Co., Korea] was used for the manipulation of plasmids and for gene cloning.

Enzymes And Chemicals

A DNeasy tissue kit (Qiagen, Netherland) was used to isolate genomic DNA from *K. pneumoniae* KCTC2242. An Axy PrepTM kit (Axygen, USA) was used to isolate bacterial plasmid DNA. A gel extraction kit (Takara, Japan, A550) was used for large-scale isolation of plasmid DNA from gels.

Plasmid Construction And Gene Deletion

Sequence data for the *budA, budB* and *budC* genes in *K. pneumoniae* KCTC2242 were provided by the National Center for Biotechnology Information (NCBI) GenBank (CP002910.1).[10] Kyung Hee University (Yongin, Korea) provided the SGSB100 strain, in which the *wabG* gene had been deleted.[9] *wabG* gene that encoding glucosyltransferase which plays a key role in the synthesis of outer core lipopolysaccharides (LPS) was inactivated to alleviate the pathogenicity of *K. pneumoniae*.

Before the deletion the *budBAC* operon, the antibiotic resistance of SGSB100 was evaluated.[5, 11] The SGSB100 strain was resistant to 500 μg/ml ampicillin, but sensitive to 50 μg/ml kanamycin. So, the SGSB109 strain was developed with a kanamycin-resistance cassette flanked by FRT and 50-bp arms homologous to both ends of the *budBAC* operon (*budBAC*FKF*budBAC*). In order to obtain a PCR fragment formed of a

kanamycine resistance cassette flanked by 34-bp of flippase recognition site (FRT, 5'-GAA GTT CCT ATT CTC TAG AAA GTA TAG G AA CTT C-3') and 50-bp of region complementary to the target sequence, two step PCR procedure was used. In the first step a 1584-bp PCR fragment containing kanamycin cassette flanked by 34-bp of flippase recognition site was generated using pKD4 as a template with primer pair FRT-Kan/Forward (5'-GAA GTT CCT ATT CTC TAG AAA GTA TAG GAA CTT CAT TCT ACC GGG TAG GGG AGG-3') and FRT-Kan/Reverse (5'-GAA GTT CCT ATA CCG CGC CGC ACA CAA AAA CCA -3'). The PCR reaction was carries out with 95^{o}C for 5 min followed by 25 cycles at 95^{o}C for 30 s, 66 ^{o}C for 55 s, and 72^{o}C for 60 s. Flippase Recognition Target (FRT) was introduced into the cassette in order to remove the kanamycin selection marker from the chromosome after disrupting the target gene. This was accomplished by transforming the cells with the FLP expression plasmid. The PCR products (FRT-flanked kanamycin-resistance gene, FCF) were ligated into the pGEM-T Easy vector (Promega, USA). Subsequently, FCF was used as the template for the PCR reaction with a primer pair containing 50-bp homologous sequences at their 5′ extremities that corresponded to both ends of *budBAC*. The sequences of the primer pair for strain SGSB100 were shown in Table 1 (homologous sequences are indicated in italics): Primer 1/forward and Primer 2/reverse. The final PCR product contained the kanamycin resistance gene flanked by FRT and 50-bp sequences homologous to both ends of the *budBAC* operon (*budBAC*FKF*budBAC*). The PCR conditions were as follows: 95°C for 5 min followed by 25 cycles at 95°C for 30 s, 65°C for 60 s, and 72°C for 60 s. Purification of plasmid DNA and PCR products was performed with a Qiagen plasmid kit (Qiagen,

Netherland) and a PCR purification kit (Qiagen, Netherland). All PCR experiments were carried out using 0.6 U of Taq polymerase (Takara, Japan).

Final PCR product was transformed through the following steps. First, SGSB100 were cultured in fresh LB medium and cells were harvested when the cultures reached to an optical density at 600 nm (O.D600) of 0.2~0.3 and washed with pre-chilled dH2O containing 10% glycerol three-times. 50 µl of cells resuspended in dH2O were mixed with 150 ng of pRedET plasmids and transferred to a pre-chilled electro-cuvette. The mixture was electroporated with a 1.8 kV, 5 msec pulse. After incubating at 30°C with shaking for an hour the electroporated cells were spread on LB agar plate supplemented with tetracycline (3 µg/ml) and incubated at 30oC overnight. The transformed *K. pneumonia* was inoculated into fresh LB media and grown to an O.D600 of 0.2~0.3 at 37 oC. Then L-arabinose was added to the culture to the final concentration of 0.5% and incubated with shaking at 37°C for an hour for the induction of Red/ET proteins. The cells were harvested and washed with pre-chilled dH2O containing 10% glycerol. Fifty µl of cells resuspended cells in dH2O were mixed with 150 ng of *budBAC*FKF*budBAC* and transferred to a pre-chilled electro-cuvette. The mixture was electroporated as described above. After incubating at 37 °C with shaking for 3 hours the electroporated cells were spread on LB agar plate supplemented with kanamycin (50 µg/ml) and incubated at 37oC overnight. Kanamycin resistant colonies were selected and *budBAC* deleted *K. pneumoniae* mutants were confirmed by colony PCR with the primer set: Forward, 5'-ATG AAT CAT TCT GCT GAA TG-3' and Reverse, 5'-TTA GTT AAA CAC CAT GCC

GC-3'. The sequences for these primer sets were complementary to the 20-base region of each homologous arm.

Culture Conditions

Stock cultures of SGSB100 and SGSB109 were grown in LB medium containing 10 g of tryptone (Difco, Detroit, MI, USA), 5 g of yeast extract (Difco), 10 g of NaCl and 50 mg of ampicillin (all in quantities per liter of deionized water at pH 7.2, unless otherwise stated) at 37°C 200 rpm for 12 hour. Media requiring solidification contained 10 g/L agar. Selection was performed in media with added kanamycin (50 mg/L). To prepare the batch culture, the stock culture was inoculated into a 2.5 L bioreactor (Kobiotech, South Korea) at 10% inoculation volume and 1 L operating volume. The stock culture and batch culture were cultivated in minimal medium containing 2 g of yeast extract, 5.25 g of dipotassium phosphate, 9.5 g of monopotassium phosphate, 6.6 g of ammonium sulfate, 0.25 g of magnesium sulfate heptahydrate, 0.05 g of ferrous sulfate heptahydrate, 0.001 g of zinc sulfate heptahydrate, 0.001 g of manganese sulfate, 0.001 g of calcium chloride dihydrate, 30 g of glucose and 50 mg of ampicillin (all in quantities per liter of deionized water at pH 7.2, unless otherwise stated).[11] In the case of SGSB109, selection was performed in media with added kanamycin (50 mg/L). Temperature of bioreactor was maintained at 37℃. Dissolved oxygen was provided by injection of filtered air at a flow rate of 1.5 vvm, and the agitation speed was maintained at 200 rpm. The pH was maintained at 5.5[5,11] through automatic addition of 5 N NaOH and 5 N HCl solutions. All batch cultures were repeated three times.

RNA Extraction, Reverse Transcription, And Real-Time PCR

Samples were withdrawn at 15h culture time and then centrifuged at 4,500 rpm for 2 min at 4°C. For total RNA extraction, 1 ml of RNAiso PLUS reagent (Takara, Japan) was added to each suspension of 5×10^6 cells. Subsequently, the resuspended cells were left at room temperature for 5 min to isolate the RNA from the nuclear protein. Subsequently, chloroform of 0.2 volume the amount of RNAiso Plus used was added to the suspension. The mixture was again allowed to stand at room temperature for 5 min and then centrifuged at 4,500 rpm for 15 min at 4°C. The top layer of the supernatant was collected, isopropanol at 0.5 times the volume of the supernatant was added, and then the mixture was allowed to stand for 10 min at room temperature. The solution was centrifuged at 4,500 rpm for 10 min at 4°C to precipitate the RNA. All of the RNA was dissolved in DEPC treated water. To digested of genomic DNA in a RNA sample the, 10 X DNaselbuffer 5µl, recombinant DNasel2 µl (Takara, Japan), ribonuclease inhibitor 20 units and DEPC-treated water up to 50 µl were added to total RNA sample 20 µg, and incubated for 30 min at 37°C. Next, we added 2.5 µl of 0.5M EDTA to sample and incubated at 80°C for 2 min. The mixture was increased reaction volume to 100 µl with DEPC treated water. Subsequently, we added 10 µl of 3M sodium acetate and 250 µl of chilled ethanol, and then mixed. The mixture kept for 20min at -80°C. Subsequently, The mixture centrifuged at 12000 rpm for 10 min at 4°C, and then removed the supernatant. Subsequently, The we washed precipitate with chilled 70% ethanol, and the mixture centrifuged at 12000 rpm for 5 min at 4°C and removed the supernatant. After drying the precipitate, it dissolved in 10 µl DEPC-treated water.

To synthesize the complementary DNA of each RNA sample, PrimeScript™ reverse transcriptase (Takara, Japan) was used. First, a mixture of isolated RNA, Oligo(dT) primer, dNTP, and RNase-free water was incubated at 65°C for 5 min. Second, PrimeScript™ reverse transcriptase, 5× PrimeScript buffer, and RNase inhibitor were added to the above solution, and the resulting mixture was incubated at 42°C for 60 min. Finally, the mixture was heated at 70°C for 15 min and then cooled on ice.

The reactant thus obtained was used as the template for the real-time RT-PCR experiment. PrimeScriptTM RT Master Mix (Takara, Japan) and a Thermal Cycler Dice Real Time System Lite (Model TP700/760, Software version: V5.0x, Takara, Japan) were used for the real time RT-PCR experiment. Primers used in the real time RT-PCR experiment are listed in Table 2. The real-time PCR was carried out with 95°C for 30 s once followed by 40 cycles at 95°C for 5 s, 60°C for 30 s, and then dissociation step once by 95°C for 15 s, 60°C for 30 s, 95°C for 15 s. To analysis for results we used ΔΔCt analysis according to the relative quantity. For positive control the housekeeping gene 16srRNA was used. And as the negative control samples without primers were used.

Carbon Distribution Analysis

The metabolic network of *K. pneumoniae* KCTC2242 was organized with glucose as a carbon substrate to include glycolysis, the pentose phosphate pathway, the citric acid cycle (TCA cycle), and the pyruvate metabolism pathway (anaerobic metabolism using pyruvate as a precursor). Basic information on the network was obtained from existing

literature[12, 13] and online databases, such as Kyoto Encyclopedia of Genes and Genomes (KEGG) and NCBI.

For dry cell weight (DCW) calculation, *K. pneumoniae* KCTC2242 Δ*wabG* batch culture samples were withdrawn at several periods (0.5 h, 2 h, 3 h, 3.5 h, 4 h, 5 h, and 7 h). The samples were centrifuged at 3736 × *g* for 10 min, and then the supernatants were discarded. To eliminate residue from culture media, 0.9% NaCl was added and the samples were recentrifuged at 3736 × *g* for 10 min. After discarding the supernatants, the precipitates were dehydrated at 55°C for 48 h. After dehydration, the mass of each sample was measured. This process was repeated at least 3 times for each sample. Based on these data, a calibration equation fitting the optical density at 600 nm and DCW changes was determined: $DCW = OD_{600} \times 0.268 - 0.0489$.

Based on the biomass composition and biosynthesis pathways of *K. pneumoniae*, determined from existing literature[13, 14], the precursor demand for biomass synthesis in *K. pneumoniae* was calculated as shown in Table 3.

Carbon distribution analysis was performed for the 15 h point in batch culture, and glucose was the sole carbon substrate. All carbon flow was calculated in proportion to total carbon substrate (C-mole of glucose). All intracellular carbon flow was calculated based on C-mole of extracellular metabolites measured by HPLC analysis and precursor demand for biomass synthesis stated above. The energy and redox balances were also included to strengthen the accuracy of the model. Pentose phosphate pathway was considered as a sole NADPH provider for biomass synthesis, and TCA cycle as a sole

ATP provider for cell energy utilizing. Also, carbon flow to CO_2 emission of each metabolic reaction was calculated. Total carbon flow to CO_2 emission was calculated by measured proportion from gas analyzer and ideal gas law.

Analytical Methods

The cell optical density (O.D.) of the culture was assayed with a spectrophotometer (Jenway, UK) at 600 nm at an appropriate dilution and was converted to the DCW. CO_2 emission was measured by gas analyzer (Lokas, Korea) directly from the off-gas of bioreactor in real-time. Gas analyzer can detect the 0~5% vol. range of CO_2 and all the measurements in this study are within this detection range.

Samples were withdrawn periodically and then centrifuged at 12470 × *g* for 10 min. The amount of carbon source, 2,3-BDO, and organic acids in the supernatants were measured on a high-performance liquid chromatography (HPLC) system using an RI2414 detector (Waters Co., USA) and an Aminex HPX-87H organic acid column (300 × 7.8 mm; Bio-Rad). Sulfuric acid solution (0.01 M) was used as the mobile phase. The temperature was 60°C and the flow rate was 0.6 ml/min. All solutions were filtered through a 0.2 μm membrane before use.

RESULTS

Elimination Of 2,3-BDO Biosynthesis Pathway In *K. Pneumoniae*

To observe the physiological role of 2,3-BDO biosynthesis, we constructed a 2,3-BDO operon deleted strain. As illustrated in Fig. 1, 2,3-BDO biosynthesis pathway is

composed of three step enzymes encoded by *budB, budA, budC* gene, respectively. Therefore, elimination of 2,3-BDO pathway can be achieved by the disruption of these genes involved in 2,3-BDO biosynthesis. These genes are presented as an operon (called *budBAC* operon) in the *K. pnuemoniae* chromosome accordingly so the *budBAC* operon deletion through homologous recombination was conducted in order to construct the SGSB 109 strain.

The deleted mutation with the *budBAC*::kan gene was confirmed by colony PCR using the primers PR1, PR2, PK1 and PK2 (Table 1). Because PR1and PR2 have SGSB100 *budBAC* operon gene sequence and the PK1 and PK2 contain the sequence for the kanamycin resistance gene (kan), the deletion mutants were confirmed by PCR with those primer sets (PR1-PK2, PK1-PR2). After selecting colonies which were sensitive to kanamycine, the *budBAC* gene was confirmed by the increased size (2400 bp) of the PCR products using the primers PR1, PR2 (Fig. 2).

Confirmation Of *Budbac* Operon Disruption In SGSB109 Strain

To confirm the *budBAC* operon disruption, the changes in gene transcription level in SGSB100 and SGSB109 were compared by real-time RT-PCR assay result. SGSB100 and SGSB109 strains were cultivated under identical growth conditions, and mRNA samples at the 15h period of mixed acid fermentation were obtained for each strain. The real-time RT-PCR results were analyzed through the ΔΔCt method using the 16srRNA gene as the reference gene. Results are presented as relative quantities (Fig. 3).

In SGSB109, all three genes in *budBAC* operon showed significant decrease at the transcription level when compared to the SGSB100 strain. From this result, we can confirm the inactivation of *budBAC* operon in the SGSB109 strain clearly.

Extracellular Metabolites Differ In *Budbac*-Deleted *K. Pneumoniae* In Batch Fermentation

Batch culture was performed with an initial concentration of 30 g/L glucose. The production of 2,3-BDO together with acetoin, ethanol, and organic acid from the culture of SGSB100 and SGSB109 were monitored. As shown in Fig. 4, SGSB100 produced 6.18 g of 2,3-BDO at 24 h, whereas SGSB109 resulted in absence of 2,3-BDO and very small amount of acetoin production. On the other hand, lactate and acetate production of SGSB109 were increased to 11.3 g/L, 2.51 g/L, which were approximately 2.3-fold and 4.1-fold higher than SGSB100, respectively. Significant increases in lactate and acetate resulted from blocking 2,3-BDO pathway. However, other organic acids and ethanol production of both strains were similar. The biomass was controlled to equivalent value in stationary phase via reduction of the yeast extract concentration. Because of excluding the difference in growth, it was possible that distribution of carbon source in metabolism was precisely identified.[15]

CO_2 Emission Assay For The SGSB100 And SGSB109 Strains

As shown in Fig. 5, CO_2 emissions of the SGSB100 and SGSB109 increased sharply to 1.15% at 3.5 h, 0.39% at 4.9 h, and then gradually decreased to 0% at 18.9 h and 15.1 h, respectively. Peak CO_2 emissions were nearly equal to emissions at the starting point of

the stationary phase. In particular, CO_2 emission by SGSB100 rapidly declined twice (once following peak CO_2 emission, and again at 18.3 h of fermentation). These changes can be accounted for by the reduction of growth and 2,3-BDO biosynthesis.

Carbon Distribution Analysis Of 2,3-BDO Biosynthesis Deficient *Klebsiella Pneumoniae*

As illustrated in Fig. 6, carbon substrate uptake in SGSB109 decreased 30.6%, compared to in SGSB100 (carbon substrate uptake: SGSB100 = 737 mmol, SGSB109 = 511 mmol). In spite of the decrease in carbon substrate uptake observed in SGSB109, the cell growth rate was similar to that of SGSB100. Thus, carbon distribution toward biomass formation was higher in SGSB109 than in SGSB100 (carbon distribution toward biomass formation: SGSB100 = 3.86%, SGSB109 = 5.24%). Because the pentose phosphate pathway and TCA cycle provide NADPH and ATP, which are essential for cell growth and biomass formation, carbon distribution toward these pathways was higher in SGSB109 than SGSB100 (carbon distribution toward the pentose phosphate pathway and TCA cycle: SGSB100 = 5.19%, 9.59% , SGSB109 = 6.85%, 11.5%).

A significant difference in the pyruvate metabolism was observed between SGSB109 and SGSB100. In SGSB100, 60.4% of the carbon substrate was allocated to production of α-acetolactate (a precursor of 2,3-BDO) from pyruvate. In SGSB109, 51.0% of the carbon substrate was allocated to lactate.

Also due to the increased carbon allocation to acetyl-CoA, acetate production was increased approximately 42.1-fold in SGSB109 relative to SGSB100. (which rarely produced acetate, at 15 h). However, nearly identical percentage (SGSB100 = 7.15%, SGSB109 = 7.33%) of carbon was allocated to ethanol biosynthesis in both strains.

Carbon allocation to CO_2 emission was decreased by 71.7%, reduced from 37.8% in SGSB100 to 10.7% in SGSB109. Reutilized and dissolved CO_2 accounts for the difference between stoichiometric CO_2 carbon distribution and measured total CO_2 carbon distribution, and this difference was reflected in CO_2 emission from acetyl-CoA synthesis.

Because pyruvate is central to cellular metabolism, the unknown carbon distribution was assumed to have been allocated to the pyruvate flux.

DISCUSSION

In this paper, we observed differences in the overall metabolism of SGSB100 and SGSB109. Extracellular metabolites analysis, gas analysis, and carbon distribution analysis were conducted to observe the metabolism of each cell.

First, observation of the extracellular metabolites produced by each type of cell showed that the pyruvate metabolism of SGSB109 was drastically altered compared to that of SGSB100.

Lactate production in SGSB109 was increased approximately 2.3-fold when compared to SGSB100 (SGSB100 = 4.97 g/L and SGSB109 = 11.3 g/L). From previous studies, it is known that the *budC* gene, which encodes acetoin reductase, plays a major role in utilizing NADH produced by the glycolysis pathway in *K. pneumoniae*. Therefore, it can be assumed that when the *budBAC* operon is disrupted, the lactate production pathway is activated to consume excess NADH resulting from non-production of 2,3-BDO.[16]

Acetate production in SGSB109 was increased approximately 4.1-fold when compared to SGSB100 (SGSB100 = 0.61 g/L and SGSB109 = 2.51 g/L). In previous studies, it has been confirmed that the expression of *budR* is enhanced by acetate-mediated induction and the a putative LysR-family transcriptional regulator derived from the *budR* gene that stimulates the expression of the 2,3-BDO operon.[17, 18] Based on the previous studies, the increased concentration of acetate in SGSB109 can be assumed as a feedback reaction due to the lack of 2,3-BDO biosynthesis. However, it is known that a typical amount of acetate biosynthesis is not favored in the cell due to several reasons such as; first acetate concentrations above 1 g/L decreases biomass production resulting in low substrate production, second acetate decreases the stability of intracellular proteins.[19] So the acetate concentration was high in SGSB109 when compared to SGSB100, but acetate was not the mainly produced alternative product in SGSB109.

A similar amount of ethanol was produced in the SGSB100 and SGSB109 strains. Although ethanol biosynthesis is an effective NADH consuming pathway, the ethanol biosynthesis appears to be less affected by the inactivation of the 2,3-BDO biosynthesis

pathway, unlike lactate biosynthesis. In mixed acid fermentation when the pH is non-controlled, ethanol may increase in SGSB109 due to the fact that it is a neutral metabolite identical to 2,3-BDO. Also, it is known from previous studies that alcohol dehydrogenase performs a unique role that prevents accumulation of toxic chemicals (acetaldehyde, reactive oxygen species) in the cell.[20] However, in previous studies it has been proven that at a pH-controlled micro-aerobic condition, ethanol is more toxic to cell growth than diol compounds (e.g. 1,3-propanediol) and lactate.[21] It has been proven that at a pH-controlled micro-aerobic condition, ethanol interacts with biological membranes, resulting a decrease in membrane integrity and this causes an increased passive flux of protons across the membrane, leading to the dissipation of the proton motive force.[22] Based on these facts, the increase of carbon distribution toward lactate in SGSB109 rather than ethanol can be explained.

Second, the overall CO_2 emissions of SGSB100 and SGSB109 were observed using a gas analyzer during a 1 L mixed acid fermentation culture. CO_2 emissions of SGSB100 and SGSB109 rapidly increased during the initial phase of cell growth. The CO_2 emission rate peak was observed during the early stationary phase of cell growth, indicating that the TCA cycle is activated at that time. The TCA cycle is a series of chemical reactions employed by all aerobic organisms to generate energy through the oxidation of acetate derived from carbohydrates, fats, and proteins into CO_2 and chemical energy in the form of adenosine triphosphate (ATP).[23] The difference in CO_2 emissions observed between SGSB100 and SGSB109 likely resulted from the presence of absence of 2,3-BDO biosynthesis, which emits CO_2.

Finally, we conducted a carbon distribution analysis and systematically visualized the overall carbon metabolism of *K. pneumoniae*. Carbon allocation to 2,3-BDO, biomass, and by-products in *K. pneumoniae* were calculated following the completion of the 1 L mixed acid fermentation. Analysis of extracellular metabolites and carbon distribution shows a radical alteration in anaerobic pyruvate metabolism when the 2.3-BDO pathway is blocked. Carbon allocation to the 2,3-BDO pathway is dominant in SGSB100, whereas in SGSB109 carbon allocation to lactate is dominant, accompanied by increased acetate production.

However, disruption of the 2,3-BDO pathway scarcely has no effect on primary metabolism (glycolysis, TCA cycle, pentose phosphate pathway, and biomass synthesis) essential for fundamental survival.

In this study, we made an effort to solve the fundamental question of why *K. pneumoniae* produces 2,3-BDO and what is the advantage of 2,3-BDO excretion in the physiological perspective in a mixed acid fermentation condition. Acidification of culture medium and redox balance in the cell are main physiological issues for the survival of the microorganisms. According to this fact, neutral metabolites, for example 2,3-BDO and ethanol, are best selection to prevent medium acidification and guarantee the suitable redox balance in the cell. However, because ethanol is more toxic than 2,3-BDO and lactate when pH is regulated, 2,3-BDO and lactate were dominantly produced in SGSB100 and SGSB109 respectively. Also, a significant increase of acetate production

was observed in SGSB109, but due to the toxicity of acetate, the increase of carbon distribution toward acetate biosynthesis had a limit. When comparing the CO_2 emission levels of SGSB100 and SGSB109, decrease in carbon allocation to CO_2 emission was observed in SGSB109 when compared to SGSB100. Also, the difference in total carbon uptake amount in SGSB100 and SGSB109 was similar to the difference in CO_2 emission levels. Based on these results, it was concluded that the 2,3-BDO pathway plays a major role in discharging CO_2 as a waste chemical of carbohydrate catabolism and activating of carbon substrate uptake of cell.

CONCLUSION

In this paper, by metabolic behavior comparison of SGSB100 and SGSB109, we observed the role and meaning of 2,3-BDO biosynthesis in *K. pneumoniae*. By comparing the SGSB109 and SGSB100 strains at a mixed fermentation condition when glucose is the carbon source, this approach sheds light on the fundamental question of why *K. pneumoniae* produces 2,3-BDO; 2,3-BDO is a neutral and non-toxic metabolite which can prevent medium acidification, 2,3-BDO synthesis is a major pathway that consumes excess NADH and regulates the redox balance, and 2,3-BDO biosynthesis facilitates carbon substrate uptake in the cell by emitting CO_2 as a waste compound.

ACKNOWLEDGMENTS

This work was supported by the R&D Program of MOTIE/KEIT (No. 10035578, Development of 2,3-Butanediol and Derivative Production Technology for C-Zero Bio-

Platform Industry). This work was also supported by the Graduate School of Specialization for Biotechnology Program of the Ministry of Knowledge Economy.

REFERENCES

1. Celińska, E.; Grajek, W. Biotechnological production of 2,3-butanediol - Current state and prospects. *Biotechnol. Adv.* 2009, 27, 715-725.

2. Ji, X.J.; Huang, H.; Ouyang, P.K. Microbial 2,3-butanediol production : A state-of-the-art review. *Biotechnol. Adv.* 2011, 29, 351-364.

3. Syu, M. J. Biological production of 2,3-butanediol. *Appl. Microbiol. Biotechnol*. 2001, 55, 10-18.

4. Guo, X.W.; Cao, C.H.; Wang, Y.Z.; Li, C.Q.; Wu, M.Y.; Chen, Y.F.; Zhang, C.Y.; Pei, H.D.; Xiao, D.G. Effect of the inactivation of lactate dehydrogenase, ethanol dehydrogenase, and phosphotransacetylase on 2,3-butanediol production in *Klebsiella pneumoniae* strain. *Biotechnol. Biofuels.* 2014, 7, 44.

5. Kim, B.R.; Lee, S.J.; Jeong, D.U.; Yang, J.M.; Oh, M.K.; Lee, J.W. Redistribution of carbon flux toward 2,3-butanediol production in *Klebsiella pneumoniae* by metabolic engineering. *PLoS ONE* 2014, 9 (10), e105322.

6. Wang, A.L.; Wang, Y.; Jiang, T.Y.; Li, L.X.; Ma, C.Q.; Xu, P. Production of 2,3-butanediol from corncob molasses, a waste by-product in xylitol production. *Appl. Microbiol. Biotechnol.* 2010, 87, 965-970.

7. Oliver, J.W.K.; Machado, L.M.P.; Yonedaa, H.; Atsumia, S. Cyanobacterial conversion of carbon dioxide to 2,3-butanediol. *PNAS*. 2013, 110, 1249-1254.

8. Köpke, M.; Mihalcea, C.; Liew, F.M.; Tizard, J.H.; Ali, M.S.; Conolly, J.J.; Sinawi, B.A.; Simpson, S.D. 2,3-Butanediol Production by Acetogenic Bacteria, an Alternative Route to Chemical Synthesis, Using Industrial Waste Gas. *Appl. Environ. Microbiol*. 2011, 77:5467-5475.

9. Jung, S.G.; Jang, J.H.; Kim, A.Y.; Lim, M.C.; Kim, B.R.; Lee, J.W.; Kim, Y.R. Removal of pathogenic factors from 2,3-butanediol-producing *Klebsiella* species by inactivating virulence-related *wabG* gene. *Appl. Microb. Biotechnol.* 2013, 5, 1997-2007.

10. Shin, S.H.; Kim, S.H.; Kim, J.Y.; Lee, S.J.; Um, Y.S.; Oh, M.K.; Kim, Y.R.; Lee, J.W.; Yang, K.S. Complete genome sequence of the 2,3-butanediol-producing *Klebsiella pneumoniae* strain KCTC 2242. *J. Bacteriol.* 2012, 194, 2736-2737.

11. Kim, B.R.; Lee, S.J.; Park, J.H.; Lu, M.S.; Oh, M.K.; Kim, Y.R.; Lee, J.W. Enhanced 2,3-butanediol production in recombinant *Klebsiella pneumoniae* via overexpression of synthesis-related genes. *J. Microbiol. Biotechnol.* 2012, 22, 1258–1263.

12. Lu, M.S.; Park, C.H.; Lee, S.J.; Kim, B.R.; Oh, M.K.; Um, Y.S.; Kim, J.W.; Lee, J.W. The regulation of 2,3-butanediol synthesis in *Klebsiella pneumoniae* as revealed by gene over-expressions and metabolic flux analysis. *Bioprocess Biosyst. Eng.* 2013, 37, 343-353.

13. Gottschalk, G. Bacterial Metabolism, 2nd ed; Springer-Verlag: New York, 1985.

14. Liao, Y.C.; Huang, T.W.; Chen, F.C.; Charusanti, P.; Hong, J.S.J.; Chang, H.Y.; Tsai, S.F.; Palsson, B.O.; Hsiung, C.A. An experimentally validated genome-scale metabolic reconstruction of *Klebsiella pneumoniae* MGH 78578, iYL1228. *J. Bacteriol.* 2011, 193 (7), 1710-1717.

15. Beltran, G.; Esteve-Zarzoso, B.; Rozes, N.; Mas, A.; Guillamon, J.M. Influence of the timing of nitrogen additions during synthetic grape must fermentations on fermentation kinetics and nitrogen consumption. *J. Agric. Food. Chem.* 2005, 53, 996-1002.

16. Xu, Y.Z.; Guo, N.N.; Zheng, Z.M.; Ou, X.J.; Liu, H.J.; Liu, D.H. Metabolism in 1,3-propanediol fed-batch fermentation by a D-lactate deficient mutant of *Klebsiella pneumonia. Biotechnol. Bioeng*. 2009, 104, 965-972.

17. Lee, S.J.; Kim, B.R.; Jeong, D.U.; Oh, M.K.; Um, Y.S.; Kim, Y.R.; Kim, J.W.; Lee, J.W. Observation of 2,3-butanediol biosynthesis in Lys regulator mutated *Klebsiella pneumoniae* at gene transcription level. *J. Biotec.* 2013, 168, 520-526.

18. Moons, P.; Houdt, R.V.; Vivijs, B.; Michiels, C.M.; Aertsen, A. Integrated regulation of acetoin fermentation by quorum sensing and pH in *Serratia plymuthica* RVH1. *Appl. Environ. Microbiol.* 2011, 77, 3422-3427.

19. Marjan, D.M.; Sofie, D.M.; Wim, S.; Erick, V. Minimizing acetate formation in *E. coli* fermentations. *J. Ind. Microbiol. Biotechnol.* 2007, 34, 689-700.

20. Kim, D.K.; Rathnasingh, C.; Song, H.H.; Lee, H.J.; Seung, D.Y.; Chang, Y.K. Metabolic engineering of a novel *Klebsiella oxytoca* strain for enhanced 2,3-butanediol production. *J. Biosci. Bioeng.* 2013, 116 (2), 186-192.

21. Cheng, K.K.; Liu, H.J.; Liu, D.H. Multiple growth inhibition of *Klebsiella pneumoniae* in 1,3-propanediol fermentation. *Biotechnol. Lett.* 2005, 27, 19-22.

22. Sikkema, J.; Bont, J.A.; Poolman, B. Mechanisms of Membrane Toxicity of Hydrocarbons. *Microbiol. Rev.* 1995, 59 (2), 201.

23. Fernie, A.R.; Carraril, F.; Lee, J.S. Respiratory metabolism : glycolysis, the TCA cycle and mitochondrial electron transport. *Curr. Opin. Plant Biol.* 2004, 7, 254-261.

Table 1. Bacterial strains and plasmids used in this study

Strain, plasmid or primer	Genotype, properties, or sequence	Source
Strains		
K. pneumoniae KCTC2242	Ap^r, *trp*R	KCTC
E. coli DH5α	F-(80d *lacZ* M15) (*lacZYA*-rgF)U1691 *hsdR17*(m+)*recA1 endA1 relA1 deoR*	RBC
SGSB100	*K. pneumoniae* KCTC2242 Δ*wabG*	Jung et al. 2013
Plasmids		
pUC18	Ap^r	Takara
pET-28a	Kan^r	Takara
pUC18K	Ap^r, pUC18 containing Kan^r from pET-28a	This study
pRedET	Tet^r, containing *gam*, *exo*, and *bet* genes	Gene Bridges
Primers[a]		
PR1	5′- ATGAATCATTCTGCTGAATGCACCTGCGAAGAGAG TCTATGCGAAACCCT*AATTAACCCTCACTAAAGGGCG* -3′	This study
PR2	5′-	This

	TtAGTTAAACACCATGCCGCCGTCGATCAGCAATGAC TGACCGGTCATATT*AATACGACTCACTATAGGGCTCGA* -3′	study
PK1	5′- ATGGGATCGGCCATTGAA-3′	This study
PK2	5′- TCAGAAGAACTCGTCAAGAAGG-3′	This study

[a]Italic letters indicate nucleotides homologous to the extremities of the kanamycin gene.

Table 2. Primers used in real-time PCR

Primer	Sequence
budB-FW	TCTCACCGATAACTTTGGCA
budB-Rev	GCCAGGTAGTACCAGAAGCC
budA-FW	GACCGACGTACTCGACGAT
budA-Rev	TTGCGGTCATCGGTAATAAA
budC-FW	ACAACATCAACGTCAAAGGG
budC-Rev	GGAACAGGCGTTGATGATTT
16srRNA-FW	AGAGTTTGATCMTGGCTCAG
16srRNA -Rev	GGTTACCTTGTTACGACTT

Table 3. Precursor for biomass synthesis in *K. pneumoniae* in μmol/gDCW

Precursor Metabolites	Requirement (μmol/g DCW)
Glucose-6-phosphate	250
Fructose-6-phosphate	149
Ribulose-5-phosphate	995
Erythrose-4-phosphate	343
Glyceraldehyde-3-phosphate	67
3-phosphoglycerate	1572
Phosphoenolpyruvate	647
Pyruvate	1114
α-Acetolactate	702
Acetyl-CoA	2407
Oxaloacetate	1847
α-ketoglutarate	1074
NADPH	16283

Fig. 1. Pyruvate metabolism in *K. pneumoniae*. Bold arrows indicate carbon flux from glucose to extracellular metabolites and open arrows indicate allocation to CO_2.

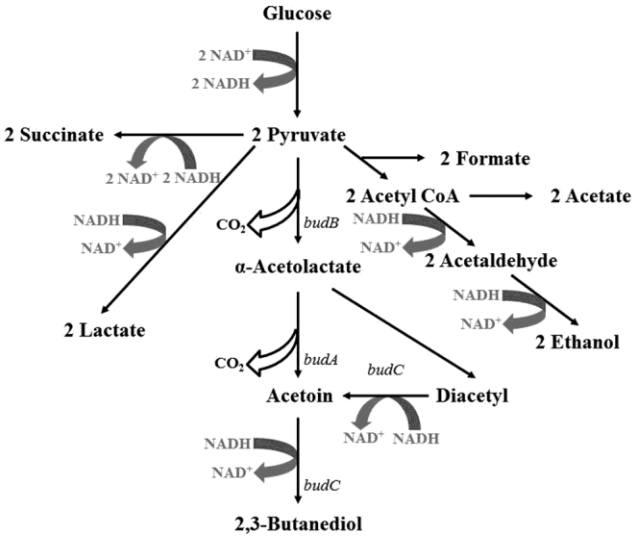

Fig. 2. Agarose gel electrophoresis of PCR products from SGSB100 and SGSB109. *budBAC* operon was disrupted from the genomic DNA of SGSB109 by inserting FRTKanFRT fragment. Lane 1: 500bp DNA marker, lane 2: SGSB100, lane3:SGSB109. The size of wild type *budBAC* operon genes is 3263bp and FRTKanFRT fragment were 1637bp.

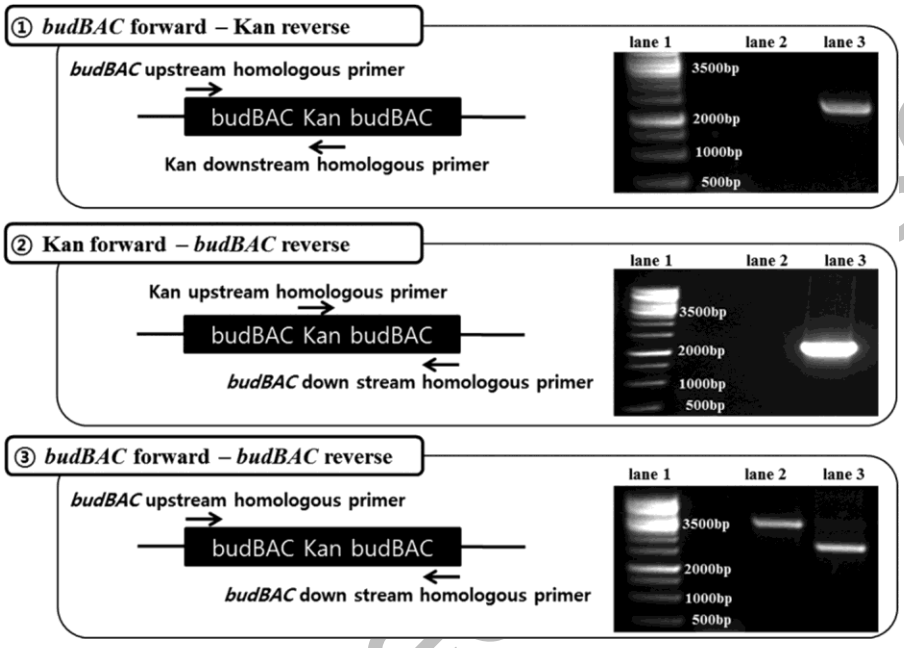

Fig. 3. Real-time PCR results for (a) *budA*, (b) *budB*, and (c) *budC* genes of *K. pneumoniae* strains SGSB100, SGSB109 15 h of batch fermentation. The abscissa and ordinate represent strains and expression levels of each gene, respectively. X = relative quantity (second derivative maximum) based on the value for the 16srRNA gene.

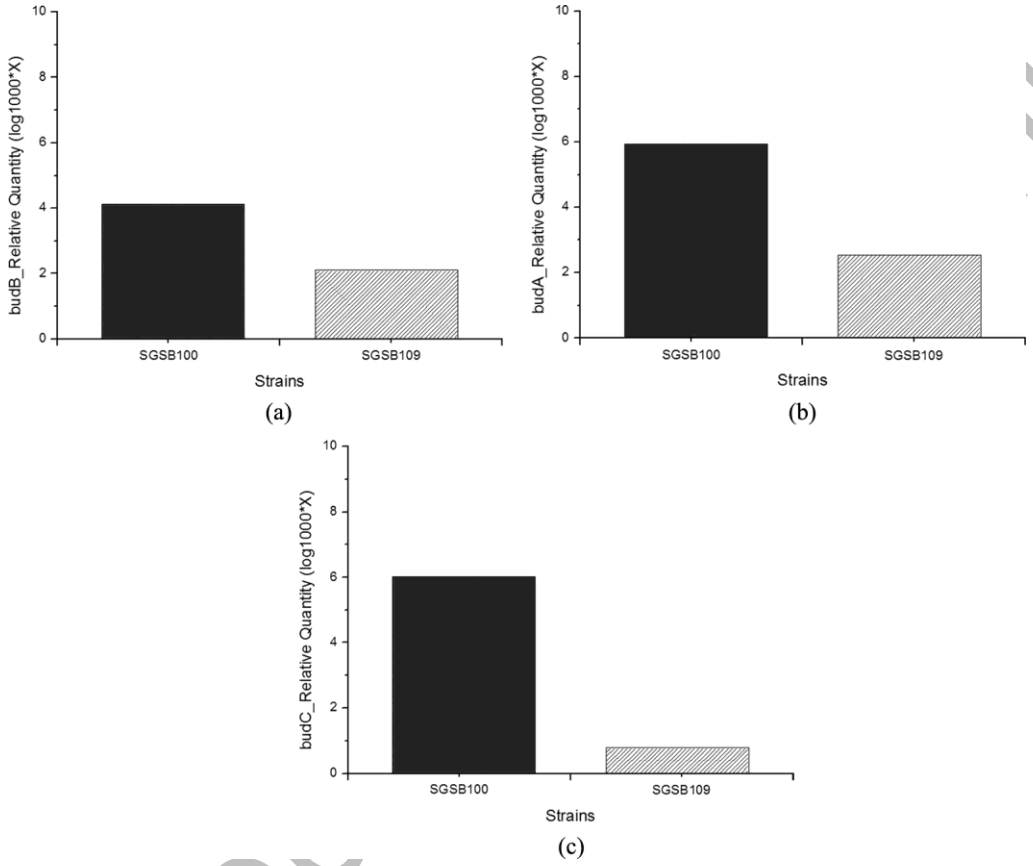

Fig. 4. (a) Cell growth (squares) and glucose consumption (circles). (b) 2,3-BDO (triangles) and lactate (inverted triangles). (c) acetoin (diamonds), acetate (pentagons), and ethanol (stars) in *K. pneumoniae* during 1L batch fermentation. Filled shapes represent SGSB100, and unfilled shapes represent SGSB109.

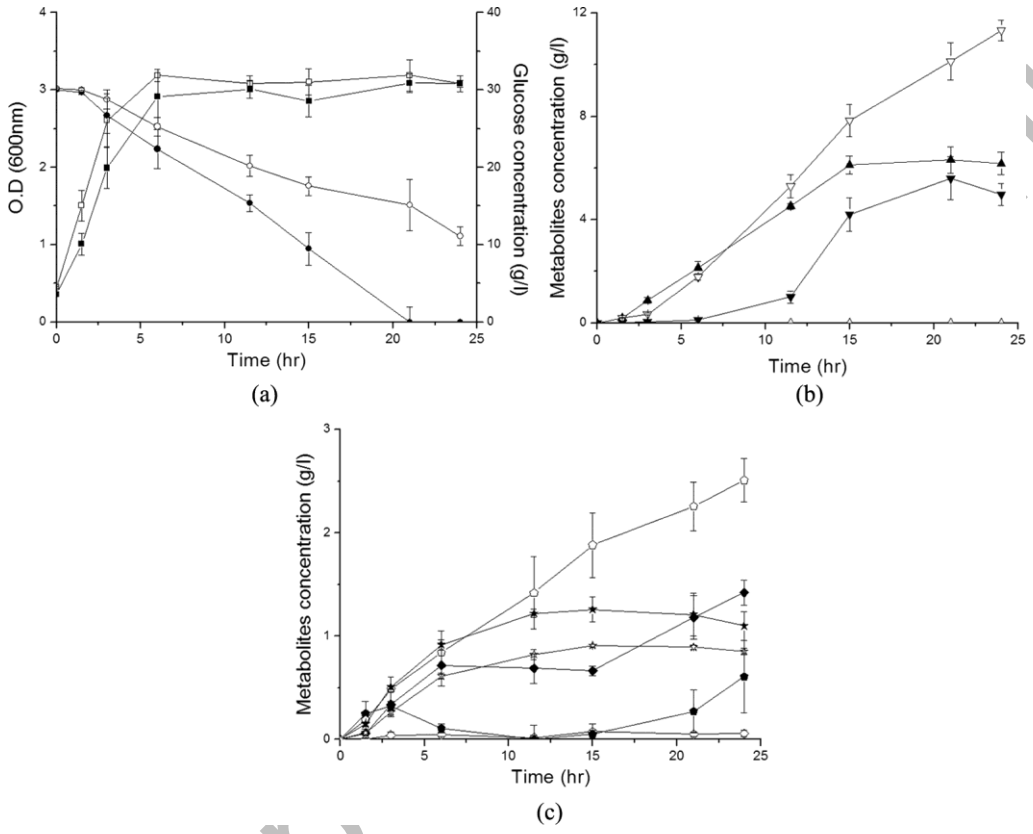

Fig. 5. The quantity of CO_2 emission is represented by the ratio in the off-gas. The bold and gray lines indicate SGSB100 and SGSB109, respectively.

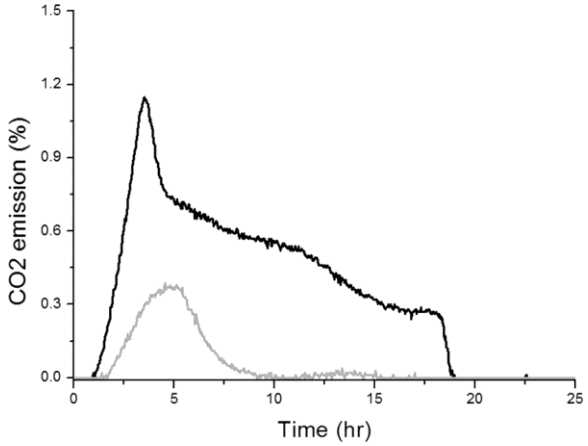

Fig. 6. Carbon distribution analysis of (a) SGSB100 and (b) SGSB109. Numbers in circles indicate the carbon number of each metabolite. Open arrows indicate carbon allocation to CO_2 and light gray arrows indicate carbon allocation to biomass formation. Carbon allocation to unknown products is indicated by dark gray arrow.